ELSEVIER

Journal of Organometallic Chemistry 506 (1996) 49–59

Journal of Organometallic Chemistry

Thermolysis of $(MeCp)_2Nb(\eta^2\text{-}CO_2)R$ complexes: decarbonylation vs. insertion

Peng-fei Fu, Masood A. Khan, Kenneth M. Nicholas *

Department of Chemistry and Biochemistry, University of Oklahoma, Norman, OK 73019, USA

Received 27 January 1995; in revised form 11 April 1995

Abstract

A series of carbon dioxide complexes of the type $Cp'_2Nb(\eta^2\text{-}CO_2)R$ ($Cp' = MeC_5H_4$; R = $-CH_2SiMe_3$, **1a**; $-CH_2CMe_3$, **1b**; $-CH_2Ph$, **1c**; $-CH_3$, **1d**) was prepared and the thermolyses of **1a–1c** investigated. When heated at 60°C in THF, complexes **1a** and **1b** are converted to the corresponding oxo derivatives $(MeC_5H_4)_2Nb(=O)R$ (**2a**, **2b**) and CO. The structure of **2a** was established by X-ray diffraction and consists of a pseudotetrahedral Cp_2MXY arrangement. That the oxo group of **2** is derived from coordinated CO_2 was confirmed by ^{13}C labeling. Thermolysis of benzyl derivative **1c** exhibits concentration dependent behavior, converting to the corresponding oxoalkyl derivative **2c** in dilute solutions but forming a mixture of **2c** and the carbonyl complex $(MeC_5H_4)_2Nb(CO)CH_2Ph$ (**4**) in more concentrated solutions. With extended reaction times **2c** and **4** decompose producing $PhCH_3$, $PhCH_2CH_2Ph$, $PhCH_2OH$, and PhCHO, the products of apparent M–C homolysis and oxidation.

Keywords: Niobium; Carbon dioxide; Decarbonylation; Insertion; Cyclopentadienyl; Alkyl

1. Introduction

Considerable interest in the reactivity of metal–carbon dioxide complexes has been evoked by the potential role of these species in metal-catalyzed transformations of carbon dioxide [1]. Transition metal-induced reactions of CO_2 include disproportionation [2], deoxygenation [3], electrophilic attack [4], oxidation of ancillary ligands [5], and insertions into M–H, M–C, M–O and M–N bonds [6]. In rather few instances, however, has it been established that a CO_2-coordinated intermediate is involved.

For several years we have sought to elucidate the reactivity of coordinated CO_2 through reactivity studies of discrete, unambiguously identified CO_2 complexes [7]. One complex of interest has been $Cp'_2Nb(\eta^2\text{-}CO_2)CH_2SiMe_3$ (**1a**, $Cp' = MeC_5H_4$) which is the only proven example of an alkyl-metal-CO_2 complex, a prospective model compound for CO_2 insertion into M–C bonds. In a preliminary study we reported the unexpected observation that **1a** undergoes thermal and photochemical decarbonylation (deoxygenation) rather than insertion, producing the oxoalkyl derivative $Cp'_2Nb(O)CH_2SiMe_3$ (**2a**, Eq. (1) [7d].) The present

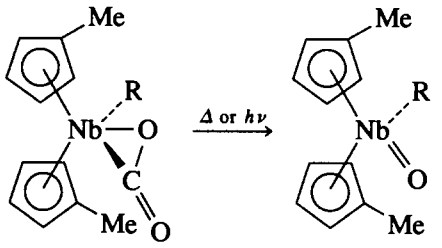

(1)

1 **2**

report expands on these initial observations to describe the preparation and thermolytic behavior of a set of complexes differing in the alkyl group on Nb. Reactivity and mechanistic studies of these reactions reveal a significant dependence of the reaction course on the nature of the alkyl group.

2. Results and discussion

2.1. Preparation of $Cp'_2Nb(CO_2)R$

To assess the effects of alkyl substitution on the properties of $Cp'_2Nb(CO_2)R$ complexes, a series of

* Corresponding author.

SSDI 0022-328X(95)05667-X

derivatives **1a–1d** was prepared using the method reported by Lappert and coworkers for **1a** (R = $CH_2Si(CH_3)_3$ [8]), i.e. sodium amalgam reduction of the corresponding alkyl chloride derivatives, $Cp'_2Nb(R)Cl$ (**3a–3d**), in the presence of CO_2 (Eq. (2)). Each of the CO_2 complexation reactions proceeds in

$$\underset{\textbf{(3a–3d)}}{Cp'_2Nb(R)Cl} + CO_2 + Na/Hg \rightarrow \underset{\begin{array}{l}\textbf{1a}\ (R=CH_2SiMe_3)\\ \textbf{1b}\ (R=CH_2CMe_3)\\ \textbf{1c}\ (R=CH_2Ph)\\ \textbf{1d}\ (R=CH_3)\end{array}}{Cp'_2Nb(\eta^2\text{-}CO_2)R} + NaCl \quad (2)$$

similarly modest yields (15%–25%), affording **1a–1d** as rather air stable, colorless crystalline solids. We note that although precursors **3a** and **3b** are available [9] by simple Grignard addition to Cp'_2NbCl_2 (Eq. (3)) the synthesis of **3c** ($R = CH_2Ph$) requires careful addition of one equivalent of $PhCH_2MgCl$ to avoid double alkylation. The corresponding methyl complex **3d** was best obtained by dialkylation of Cp'_2NbCl_2 with CH_3MgCl followed by monodemethylation with $PbCl_2$ (Eqs. (4)(5)).

$$Cp'_2NbCl_2 + RMgX \rightarrow Cp'_2Nb(R)Cl\ (\textbf{3a–3c}) + MgXCl \quad (3)$$

$$Cp'_2NbCl_2 + 2MeMgX \rightarrow Cp'_2NbMe_2 + MgX_2 \quad (4)$$

$$Cp'_2NbMe_2 + PbCl_2 \rightarrow Cp'_2Nb(Me)Cl\ (\textbf{3d}) \quad (5)$$

Compounds **1a–1d** all exhibit IR spectra indicative of the presence of coordinated CO_2 in the η^2-mode [10] with a strong IR band for the C=O stretch at approximately 1700 (± 5) cm^{-1} (KBr) and weaker bands associated with C–O stretching and bending modes (Table 1); these bands for complexes **1a**, **1b** exhibited appropriate isotopic shifts when derived from $^{13}CO_2$. The ^1H NMR and ^{13}C NMR data for **1a–1c** further support this formulation exhibiting a characteristic, ^{13}C NMR absorption for complexed CO_2 at 200.9 and 200.6 ppm for **1a** and **1c** respectively. These values are in the same range, 200–210 ppm [11], as found for the few other X-ray proven η^2-CO_2 complexes. Finally, this assignment has been unambiguously established by X-ray diffraction in the case of **1c** (Tables 2–4) [12]. The structure of **1c** (Fig. 1), like its relative **1a** [9], has the η^2-CO_2 and alkyl ligands in the equatorial plane bisecting the Cp′–Nb–Cp′ angle and the C=O group of the CO_2 ligand projecting away from the alkyl group (''outside''). This feature is common to related Cp_2MX-ketene complexes [13] and appears to be the sterically less hindered arrangement, although electronic factors may also play a role. The corresponding bond angles and lengths in the two complexes are quite similar, showing little effect of the different alkyl ligands except for the distinctly longer Nb–CH_2R bond of the benzyl derivative **1c** (2.337(4) vs. 2.282(11) Å for **1a**).

Table 2
Crystal data for **1c** and **2a**

	1c	**2a**
Formula	$C_{20}H_{21}NbO_2$	$C_{16}H_{25}NbOSi$
Molecular weight ($g\ mol^{-1}$)	386.3	354.37
Temperature (°C)	−110	−110
a (Å), α (deg)	6.938(2), 94.46(3)	6.104(2)
b (Å), β (deg)	10.234(4), 92.80(3)	11.564(3)
c (Å), γ (deg)	12.227(5), 109.60(3)	23.064(5)
V (Å^3)	812.8	1628.0
Space group	$P1$	$P2_12_12_1$
Z	2	4
Density ($g\ cm^{-3}$)	1.578	1.446
λ(Mo Kα) (Å)	0.71069	0.71069
μ(Mo Kα) (cm^{-1})	6.8	7.84
F(000)	396	712
Data collection range (deg)	53	55
Total reflections measured	3338	2184
Reflections used [$I > 2\sigma(I)$]	2300	1815
R	0.030	0.022
R_w	0.033	0.022
GOF	1.1	1.016

$R = \Sigma\,||F_o| - |F_c||/\Sigma|F_o|$. $R_w = [\Sigma w(|F_o| - |F_c|)^2/\Sigma wF_o^2]^{1/2}$. GOF $= [\Sigma w|F_o| - |F_c|)^2/(m-n)]^{1/2}$

2.2. *Thermolysis of $Cp'_2Nb(CO_2)R$*

Although the complexes $Cp'_2Nb(\eta^2\text{-}CO_2)R$ (**1**) are remarkably stable under ambient conditions, when heated at 60°C (10^{-2}–10^{-3} M in THF) **1a–1c** are consumed gradually leading to somewhat air-sensitive products **2a–2c** as white solids (20%–40%) after sublimation. Uncharacterized insoluble materials (polymeric)

Table 1
IR assignments for coordinated CO_2 in **1a** and **1c**

Compound, $\Delta\nu$	ν(C=O)	ν(C–O)	δ(O–C–O)	γ(C=O)
$Cp'_2Nb(^{12}CO_2)CH_2SiMe_3$	1697	1166, 1119	726	567
$Cp'_2Nb(^{13}CO_2)CH_2SiMe_3$	1654	1148, 1093	715	545
$\Delta\nu$	43	18, 26	11	22
$Cp'_2Nb(^{12}CO_2)CH_2Ph$	1704	1164, 1122	732	571
$Cp'_2Nb(^{13}CO_2)CH_2Ph$	1659	1144, 1095	720	553
$\Delta\nu$	45	20, 27	12	18

Table 3
Atomic coordinates for non-hydrogen atoms for **1c**

Atom	x	y	z
Nb(1)	0.09243(6)	0.29268(4)	0.22966(3)
O(1)	0.4028(4)	0.2893(3)	0.2253(2)
O(2)	0.5571(4)	0.5187(3)	0.2910(2)
C(1)	0.4126(6)	0.4137(4)	0.2607(3)
C(2)	0.0347(6)	0.0620(4)	0.1610(3)
C(11)	0.1433(6)	0.2509(4)	0.4222(3)
C(12)	0.1354(7)	0.3867(4)	0.4196(3)
C(13)	−0.0623(7)	0.3750(4)	0.3761(3)
C(14)	−0.1774(6)	0.2319(4)	0.3512(3)
C(15)	−0.0498(6)	0.1565(4)	0.3801(3)
C(16)	0.3209(8)	0.2140(7)	0.4667(4)
C(21)	0.1425(6)	0.3510(4)	0.0394(3)
C(22)	0.1641(6)	0.4744(4)	0.1081(3)
C(23)	−0.0253(6)	0.4613(4)	0.1507(3)
C(24)	−0.1669(6)	0.3274(4)	0.1094(3)
C(25)	−0.0630(6)	0.2621(4)	0.0407(3)
C(26)	0.3038(7)	0.3218(5)	−0.0245(4)
C(31)	0.1285(6)	−0.0292(4)	0.2158(3)
C(32)	0.0157(7)	−0.1345(4)	0.2778(3)
C(33)	0.1014(8)	−0.2230(5)	0.3257(4)
C(34)	0.3018(8)	−0.2119(5)	0.3097(4)
C(35)	0.4161(7)	−0.1097(5)	0.2476(4)
C(36)	0.3312(6)	−0.0201(4)	0.2017(4)

were also obtained whose mass spectra exhibited prominent peaks corresponding to $[Cp'_2Nb(O)R]^+$ and $[Cp'_2NbO]^+$. The complexes **2a–2c** have no significant IR absorption in the 1600–2000 cm^{-1} region as expected for a carboxylate or metalloester insertion product. Instead, a strong peak in the region of 800–840 cm^{-1}, corresponding MS molecular ions, and supporting ^1H and ^{13}C NMR spectra, together with elemental analysis, led us to identify **2a–2c** as oxoalkyl derivatives $Cp'_2Nb(O)R$ (Eq. (1)). The ^1H NMR spectra of **2a–2c** display appropriate resonances for the $-SiMe_3$, Cp– and Cp–Me groups. The signal of the methylene protons of the $-CH_2R$ group of **2a–2c** is substantially shielded (0.3–0.7 ppm) relative to the CO_2 complexes, while the corresponding Cp′ resonances are deshielded (approximately 0.3–0.6 ppm), probably caused by an increase in polar character in the Nb–C bond and an increase in the oxidation state of the metal atom in proceeding from **1** to **2**.

This assignment was confirmed by a single-crystal X-ray structure determination of **2a** (Fig. 2, Tables 2, 5, 6). The structure of **2a**, one of a small number of characterized oxo-alkyl complexes [14], consists of a pseudotetrahedral Cp'_2MXY arrangement with a Cp′(1)–Nb–Cp′(2) angle (131.0°), typical of bent sandwich compounds without restrictive tethers or large steric effects. The Nb=O bond distance (1.741 Å) is similar to that in $(C_5H_4SiMe_3)_2Nb(O)Me$, (1.720(7) Å), but is significantly longer than in $Cp_2Nb(O)$-$[C_7H_5(CF_3)_2]$ (1.63(3) Å) [15] and typical M=O bonds of other transition metal complexes (1.59 A to 1.66 Å) [14]. This effect is consistent with a somewhat electron-rich niobium center in **2a** with diminished $O_\pi \rightarrow Nb_\pi$ bonding and the Lewis base character of the

Table 4
Bond lengths (Å) and angles (deg) for **1c**

Atom–Atom–Atom	Distance angle	Standard deviation
Nb1–O1	2.16838	0.00251
Nb1–C1	2.14742	0.00380
Nb1–C2	2.33726	0.00374
Nb1–CP1	2.09548	0.00383
Nb1–CP2	2.10276	0.00385
O1–C1	1.29031	0.00439
O2–C1	1.21448	0.00459
C2–C31	1.48471	0.00520
C11–C12	1.41271	0.00612
C11–C15	1.40701	0.00571
C11–C16	1.49450	0.00711
C12–C13	1.40989	0.00598
C13–C14	1.41333	0.00574
C14–C15	1.40477	0.00562
C21–C22	1.42108	0.00518
C21–C25	1.41226	0.00534
C21–C26	1.49216	0.00570
C22–C23	1.40511	0.00568
C23–C24	1.42841	0.00590
C24–C25	1.40161	0.00561
C31–C32	1.40366	0.00538
C31–C36	1.39754	0.00557
C32–C33	1.38716	0.00593
C33–C34	1.38198	0.00735
C34–C35	1.38684	0.00693
C35–C36	1.38388	0.00631
O1–Nb1–C1	34.788	0.1175
O1–Nb1–C2	78.172	0.1203
O1–Nb1–CP1	111.037	0.1248
O1–Nb1–CP2	110.613	0.1245
C1–Nb1–C2	112.955	0.1407
C1–Nb1–CP1	101.400	0.1424
C1–Nb1–CP2	101.842	0.1429
C2–Nb1–CP1	104.837	0.1422
C2–Nb1–CP2	101.545	0.1415
CP1–Nb1–CP2	134.174	0.1498
Nb1–O1–C1	71.720	0.2005
Nb1–C1–O1	73.492	0.2005
Nb1–C1–O2	154.525	0.2932
O1–C1–O2	131.955	0.3558
Nb1–C2–C31	122.656	0.2582
C12–C11–C15	107.425	0.3600
C12–C11–C16	126.190	0.4168
C15–C11–C16	126.320	0.4280
C11–C12–C13	108.038	0.3679
C12–C13–C14	108.200	0.3627
C13–C14–C15	107.361	0.3428
C11–C15–C14	108.975	0.3608
C22–C21–C25	106.861	0.3255
C22–C21–C26	126.766	0.3533
C25–C21–C26	126.352	0.3429
C21–C22–C23	108.771	0.3414
C22–C23–C24	107.586	0.3462
C23–C24–C25	107.545	0.3500
C21–C25–C24	109.225	0.3404
C2–C31–C32	122.112	0.3506
C2–C31–C36	121.191	0.3428

Table 4 (continued)

Atom–Atom–Atom	Distance angle	Standard deviation
C32–C31–C36	116.564	0.3492
C31–C32–C33	122.122	0.4123
C32–C33–C34	119.878	0.4238
C33–C34–C35	119.192	0.4232
C34–C35–C36	120.702	0.4371
C31–C36–C35	121.509	0.3950

oxo group of **2a** in its interaction with $ZnCl_2$ and $LiPF_6$ [7f].

Interestingly, the outcome of thermolysis of $Cp'_2Nb(\eta^2\text{-}CO_2)CH_2Ph$ (**1c**) was found to be concentration dependent. In more dilute solutions, e.g. $\leqslant 8 \times 10^{-3}$ M, **1c**, like **1a** and **1b**, undergoes decarbonylation at 60°C yielding the corresponding oxo complex **2c** (25%). At higher concentrations, however, e.g. $(3\text{–}5) \times 10^{-2}$ M, **1c** is converted to a mixture of **2c** and the corresponding green carbonyl complex, $Cp'_2Nb(CO)CH_2Ph$ (**4c**), after about 4 h (Eq. (6)).

$$Cp'_2Nb(\eta^2\text{-}CO_2)CH_2Ph\ (\mathbf{1c}) \rightarrow Cp'_2Nb(O)CH_2Ph\ (\mathbf{2c}) + Cp'_2Nb(CO)CH_2Ph\ (\mathbf{4c}) + CO + CO_2 \quad (6)$$

The latter was characterized by the presence of an intense IR absorption at 1889 cm^{-1} and supporting NMR and MS data. This assignment was confirmed by comparison of the spectroscopic data with an authentic sample prepared independently from the reduction of $Cp'_2Nb(Cl)CH_2Ph$ with sodium amalgam under a carbon monoxide atmosphere (Eq. (7)).

$$Cp'_2Nb(Cl)CH_2Ph + CO + Na/Hg \rightarrow Cp'_2Nb(CO)CH_2Ph + NaCl \quad (7)$$

Thermolysis of $Cp'_2Nb(\eta^2\text{-}^{13}CO_2)CH_2Ph$ (**1c**) under these conditions revealed the coproduction of both ^{13}CO and $^{13}CO_2$ (vide infra).

When the thermolysis of **1c** (2.59×10^{-2} M) was allowed to proceed until the starting materials were totally consumed, no $Cp'_2Nb(CO)CH_2Ph$ (**4c**) and only a small amount of $Cp'_2Nb(O)CH_2Ph$ (**2c**) were detected spectroscopically. The IR spectrum of the solution revealed instead two new carbonyl absorptions at 1723 cm^{-1} and 1778 cm^{-1}, which are assigned to benzaldehyde and butyrolactone, respectively, when supported by ^1H NMR and GC/MS data (Eq. (8)). GC/MS analysis of the solution also indicated the formation of

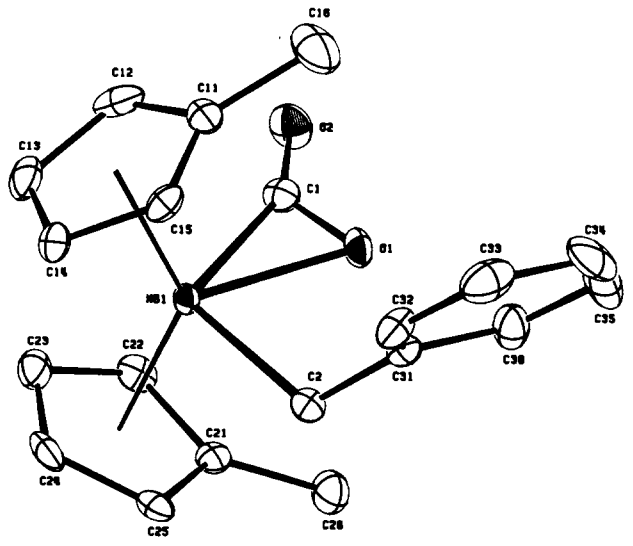

Fig. 1. ORTEP diagram of **1c** with hydrogen atoms omitted for clarity.

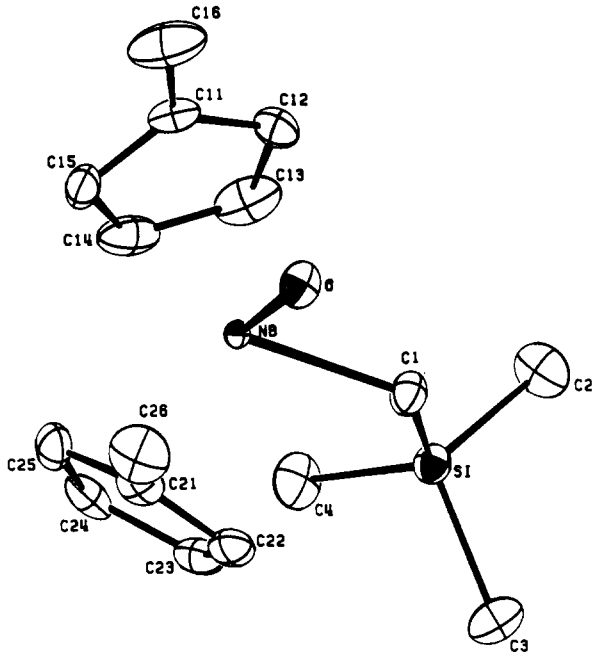

Fig. 2. ORTEP diagram of **2a** with hydrogen atoms omitted for clarity.

Table 5
Atomic coordinates for the non-hydrogen atoms for **2a**

Atom	x	y	z
Nb	0.19631(5)	0.31406(2)	0.84216(1)
Si	0.20090(21)	0.56314(7)	0.94454(4)
O	0.4420(4)	0.2560(2)	0.8173(1)
C(1)	0.3412(6)	0.4516(3)	0.8992(2)
C(2)	0.2969(10)	0.5524(4)	1.0214(2)
C(3)	0.2721(9)	0.7096(3)	0.9163(2)
C(4)	−0.1059(7)	0.5570(4)	0.9470(2)
C(11)	0.1529(6)	0.1145(3)	0.8803(1)
C(12)	0.2248(7)	0.1836(4)	0.9262(1)
C(13)	0.0613(9)	0.2620(3)	0.9399(2)
C(14)	−0.1132(8)	0.2452(3)	0.9032(2)
C(15)	−0.0539(7)	0.1564(3)	0.8645(2)
C(16)	0.2824(12)	0.0188(3)	0.8521(2)
C(21)	0.1630(6)	0.3587(3)	0.7358(1)
C(22)	0.2146(8)	0.4632(3)	0.7638(2)
C(23)	0.0385(7)	0.4950(3)	0.7997(1)
C(24)	−0.1232(7)	0.4106(4)	0.7954(2)
C(25)	−0.0432(6)	0.3231(4)	0.7577(1)
C(26)	0.3056(10)	0.2951(4)	0.6940(2)

Table 6
Bond lengths (Å) and angles (deg) for **2a**

Atom–atom–atom	Distance angle	Standard deviation
Nb–O	1.74070	0.00259
Nb–C1	2.24588	0.00365
Nb–CP1	2.16555	0.00366
Nb–CP2	2.18299	0.00372
Nb–C11	2.48390	0.00327
Nb–C12	2.46194	0.00379
Nb–C13	2.47470	0.00403
Nb–C14	2.48729	0.00455
Nb–C15	2.43344	0.00401
Nb–C21	2.51467	0.00337
Nb–C22	2.50050	0.00350
Nb–C23	2.50305	0.00366
Nb–C24	2.49291	0.00391
Nb–C25	2.43776	0.00349
Si–Cl	1.86812	0.00376
Si–C2	1.87200	0.00423
Si–C3	1.86606	0.00391
Si–C4	1.87523	0.00447
C11–C12	1.39564	0.00505
C11–C15	1.40048	0.00566
C11–C16	1.50769	0.00619
C12–C13	1.38603	0.00644
C13–C14	1.37441	0.00661
C14–C15	1.40779	0.00565
C21–C22	1.40666	0.00495
C21–C25	1.41672	0.00528
C21–C26	1.49295	0.00591
C22–C23	1.40613	0.00582
C23–C24	1.39225	0.00560
C24–C25	1.41985	0.00538
C1–H011	0.96028	0.04404
C1–H012	0.88694	0.05046
C2–H021	0.89885	0.04027
C2–H022	0.78493	0.06456
C2–H023	1.02394	0.06741
C3–H031	0.95311	0.03543
C3–H032	0.97253	0.06087
C3–H033	0.94535	0.04266
C4–H041	0.98471	0.05323
C4–H042	1.02735	0.06207
C4–H043	0.95075	0.05896
C12–H12	0.92641	0.04795
C13–H13	0.90024	0.04762
C14–H14	0.91513	0.04134
C15–H15	0.86387	0.03754
C16–H161	1.04597	0.06341
C16–H162	1.06246	0.05424
C16–H163	1.00748	0.06277
C22–H22	0.93437	0.04736
C23–H23	1.01411	0.03919
C24–H24	0.97582	0.04233
C25–H25	0.86869	0.03929
C26–H261	1.05966	0.06228
C26–H262	0.96136	0.05542
C26–H263	1.04306	0.06150
O–Nb–C1	97.322	0.1237
O–Nb–CP1	107.873	0.1241
O–Nb–CP2	107.407	0.1281
C1–Nb–CP1	103.360	0.1386
C1–Nb–CP2	104.138	0.1313
CP1–Nb–CP2	131.022	0.1398

Table 6 (continued)

Atom–atom–atom	Distance angle	Standard deviation
C1–Si–C2	109.945	0.2032
C1–S1–C3	108.934	0.1881
C1–Si–C4	116.675	0.1853
C2–Si–C3	108.551	0.2070
C2–Si–C4	106.320	0.2376
C3–Si–C4	106.109	0.2172
Nb–C1–Si	129.528	0.1928
C12–C11–C15	106.427	0.3271
C12–C11–C16	125.582	0.3989
C15–C11–C16	127.903	0.3712
C11–C12–C13	108.761	0.3692
C12–C13–C14	108.916	0.3516
C13–C14–C15	107.139	0.3909
C11–C15–C14	108.602	0.3525
C22–C21–C25	106.543	0.3345
C22–C21–C26	126.113	0.3861
C25–C21–C26	127.251	0.3564
C21–C22–C23	108.906	0.3702
C22–C23–C24	108.422	0.3205
C23–C24–C25	107.448	0.3332
C21–C25–C24	108.488	0.3380
C11–C12–H12	123.742	2.9840
C13–C12–H12	127.396	3.0307
C12–C13–H13	129.102	3.1463
C14–C13–H13	121.971	3.1422
C13–C14–H14	123.852	2.5032
C15–C14–H14	128.842	2.5038
C11–C15–H15	122.383	2.5514
C14–C15–H15	128.970	2.5703
C11–C16–H161	106.790	3.5534
C11–C16–H162	103.028	3.1195
C11–C16–H163	103.094	3.3366
H161–C16–H162	118.087	4.5193
H161–C16–H163	124.843	4.8787
H162–C16–H163	98.278	4.7662
C21–C22–H22	127.291	2.7946
C23–C22–H22	123.787	2.7887
C22–C23–H23	128.476	2.3278
C24–C23–H23	123.026	2.3362
C23–C24–H24	128.303	2.1849
C25–C24–H24	124.220	2.1829
C21–C25–H25	125.158	2.6037
C24–C25–H25	126.343	2.6102
C21–C26–H261	110.118	3.2364
C21–C26–H262	110.988	3.2715
C21–C26–H263	112.406	3.0812
H261–C26–H262	105.095	4.4532
H261–C26–H263	113.184	4.8093
H262–C26–H263	104.683	4.4588

benzyl alcohol, 1,2-diphenylethane, and toluene. That the oxygen in the organic products is derived from CO_2 was established by thermolysis of $Cp'_2Nb(\eta^2\text{-}C^{18}O_2)CH_2Ph$.

$$Cp'_2Nb(CO_2)CH_2Ph \xrightarrow[\text{THF}]{\Delta,\ \text{high } c,\ 35\ \text{h}} \text{Ph(C=O)H} + \text{(cyclic ester)} + \text{Ph(CH}_2\text{)OH} + \text{PhCH}_2\text{CH}_2\text{Ph} + \text{PhCH}_3 \quad (8)$$

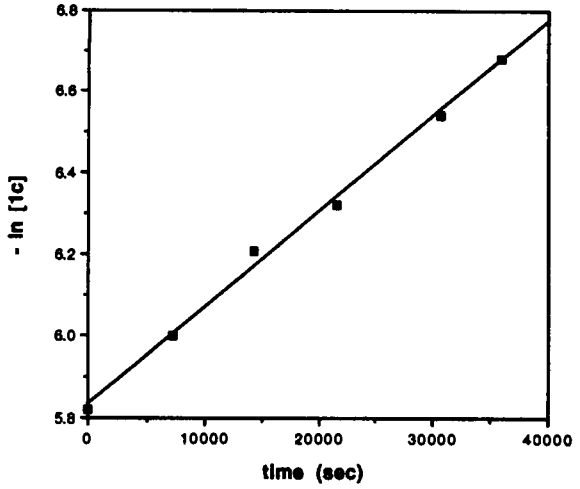

Fig. 3. First-order plot of thermolysis of **1c** in THF at 60°C, $c_i = 6.9 \times 10^{-3}$ M.

Since these species appear late in the thermolysis, we suggest that they are secondary products arising from decomposition of the oxo and carbonyl complexes **2c**, **3c**. Long-term heating probably results in homolytic cleavage of the Nb–CH_2Ph bond of **2c** and **4c**. The benzyl radical thus produced can undergo dimerization to generate $PhCH_2CH_2Ph$ or hydrogen atom abstraction from solvent (THF) to give $PhCH_3$; the remaining THF free radical may then abstract oxygen from the Nb=O fragment to yield butyrolactone. The compounds PhCHO and $PhCH_2OH$ are probably produced either by rupture of the Nb–CH_2Ph bond with concomitant oxygen transfer or intramolecular migration of the benzyl group to the oxo ligand followed by decoordination.

2.3. Mechanistic studies

Kinetic measurements of the thermolyses of **1a–1c** were conducted at 60°C in THF with IR (1740 cm^{-1}) and/or NMR monitoring of the disappearance of the CO_2 complex. At starting concentrations less than 8×10^{-2} M each of the compounds is consumed by a first-order process (2–3 half lives) with the following rate constants: **1a**, $k = 4.0 \pm 0.4 \times 10^{-5}$ s^{-1}; **1b**, $4.0 \pm 0.4 \times 10^{-5}$ s^{-1}; **1c**, $k = 2.0 \pm 0.4 \times 10^{-5}$ s^{-1} (Fig. 3). Under these conditions no intermediate species were detected and the oxoalkyl complexes **2a–2c** were the major products. The decarbonylation reaction is essentially irreversible for when the oxoalkyl complex **2a** was pressurized with up to 5 atm of CO in THF no conversion back to the CO_2 complex **1a** occurred after 3 h.

The simplest mechanistic explanation for the above results is the operation of a concerted decarbonylation process with cleavage of the Nb–C and C–O bonds simultaneously with formation of the Nb–O and C–O bonds. Bond energy (Nb–O > Nb–C and $C–O_\sigma > C–O_\pi$) and entropic considerations suggest that this process is thermodynamically favored. Its irreversible nature is supported by the non-convertibility of **2** to **1** with CO. Preliminary extended Hückel MO calculations [16] indicate that the CO extrusion reaction of $Cp_2Nb(\eta^2\text{-}CO_2)R$ is also kinetically favorable with no symmetry imposed barrier. The rate of decarbonylation of **1** is rather insensitive to the alkyl substituent with the benzyl complex **1c**, exhibiting a small but significantly diminished rate. It is unclear whether this modest effect is steric or electronic in origin. Limited thermodynamic data [17] suggest that the Nb–CH_2Ph bond is weaker than the Nb–CH_2SiMe_3 and Nb–CH_2CMe_3 bonds which could strengthen the Nb–CO_2 interaction of **1c**, but there is no evidence of this from comparison of the X-ray structure or IR spectra of **1a** and **1c**. Alternatively, the somewhat greater reactivity of **1a**, **1b**, which have bulkier alkyl ligands, could reflect a greater steric strain which is relieved in the decarbonylation process.

As was noted earlier, at higher concentrations thermolysis of **1c** (but not **1a** and **1b**) produces both oxoalkyl derivative **2c** and carbonyl complex **3c**. Monitoring these reactions by NMR revealed that (1) the disappearance of **1c** does not conform to simple first- or second-order kinetic behavior, (2) the carbonyl complex **4c** is initially formed at a slower rate than the oxoalkyl derivative **2c** with the induction period being shortened at higher concentrations of **1c**, and (3) no intermediates could be detected. These observations suggest that the carbonyl derivative **4c** is a secondary product of the thermolysis of **1c**.

To obtain additional insight into the mechanism of the reaction, thermolysis of isotopically labeled $Cp'_2Nb(\eta^2\text{-}^{13}CO_2)CH_2Ph$ (**1c***) was conducted. An NMR tube sealed under nitrogen containing **1c*** in THF-d_8 was heated at 60°C and monitored by ^1H NMR. After 15 h $Cp'_2Nb(O)CH_2Ph$ (**2c**) and $Cp'_2Nb(^{13}CO)CH_2Ph$ (**4c***) were formed in about a 60:40 mixture. The ^{13}C NMR spectrum of this sample showed that free CO_2 (128.8 ppm) had formed but free CO was not detected, probably because of its limited solubility in THF (confirmed separately). However, when the thermolysis of **1c** was carried out in refluxing $CDCl_3$ at 60°C, the same reaction occurred and a strong peak at 185 ppm, corresponding to free CO, was found. Further evidence that CO_2 dissociation is involved in the thermolysis of **1c** comes from the observation of the color change from colorless to purple, typical for $Cp_2Nb(III)X$ derivatives, which occurs during the thermolysis. Apparently, the dissociation of CO_2 from **1c** is a parallel process to its decarbonylation. Interestingly, heating **1c** in concentrated THF solution under 1 atm CO caused no increase in the rate of formation of Nb–CO.

At least two plausible mechanisms can account for the formation of the carbonyl complex **4c** in the ther-

molysis of **1c** at higher concentrations (Schemes 1A,B). In the first, dissociation of CO_2 from **1c** produces a coordinatively unsaturated 16-electron species **5**, which traps CO generated from competing decarbonylation of **1c** (Scheme 1A). An alternative mechanism also involves dissociation of CO_2 to form **5**, which then acts as a Lewis acid to attack the coordinated CO_2 of another molecule of **1c**; the resulting μ-CO_2 intermediate **6** then cleaves to give **2c** and **4c** (Scheme 1B). An analogous bridging CO_2 complex has been observed in the reaction of **1a** with $ZnCl_2$ [7f]. A higher starting concentration of **1c** would increase the concentration of 16 electron intermediate **5**, enhancing the likelihood of its trapping by free CO or by available starting material **1c**; at lower concentrations of **1c**, trapping of **5** would be less effective, leading to domination by the irreversible, unimolecular decarbonylation channel.

Although both mechanisms reasonably account for the products, the former is inconsistent with the observed non-first-order kinetic behavior at higher concentrations of **1c** and the lack of an effect of added CO on the formation of carbonyl complex **4c** since both direct decarbonylation and dissociation of CO_2 from **1c** are likely to be slow relative to CO trapping by **5**. We therefore favor Scheme 1B in which intermediate **5** reacts faster with **1a** than with free CO. This seems reasonable because of the higher concentration of **1** relative to that of sparingly soluble CO. If this step or the subsequent decomposition of bridged intermediate **6** is rate determining, the observed kinetics would be accommodated.

How can one explain the unique behavior of **1c** vis-a-vis **1a** and **1b**, i.e. its conversion to both carbonyl and oxo derivatives at higher concentrations? We suggest that this effect may either be related to the steric differences among their alkyl ligands or to the unique ability of the benzyl derivative to coordinate in the η^3-fashion [18]. The presence of the smaller alkyl group in the benzyl complex **1c** may facilitate its succeeding combination with the 16 electron species Cp'_2Nb-(CH_2Ph) leading to formation of the μ-CO_2 complex **6** which is prerequisite to formation of the carbonyl complex **4**. This association may be suppressed for the bulkier complexes **1a**, **1b**, inhibiting formation of the CO complexes in these cases. Alternatively, in the case of **1c**, formation of intermediate **5** could be favored through its stabilization by η^3-coordination of the benzyl unit, providing an 18 electron count.

Although metal-oxo and -oxide complexes [3] have been observed previously in the reactions of CO_2 with metal complexes, the reactions described herein provide the first unequivocal examples of thermal "CO_2 splitting" to M–O and CO from coordinated CO_2. This process parallels the scission of other η^2-unsaturated ligands such as RN=O [19] and RNC=O [20] bound to Cp_2Nb-X units. It is interesting to contrast these results

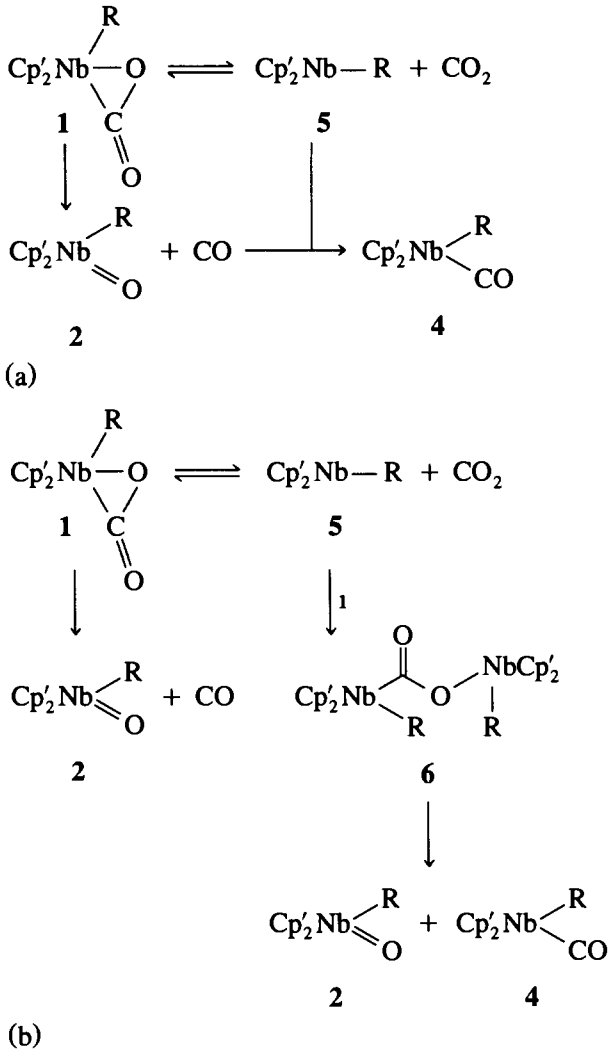

Scheme 1.

with the thermal and photoinduced reductive disproportionation (to CO and CO^{2-} d3) which is found for the isoelectronic, structurally related $Cp_2Mo(\eta^2$-$CO_2)$ [7a] and for other complexes of the later transition metals [2]. The partitioning between these two pathways reflects the relative oxophilicity of the earlier vs. the later transition metals.

Finally, we conclude by raising the question, why decarbonylation and not insertion? As discussed earlier it is likely that the decarbonylation reaction is itself thermodynamically favorable, i.e. has a negative ΔG. However, the isolability of a related niobium carboxylate, $Cp_2Nb(\eta^2$-$O_2CR)$ [21], and crude bond energy estimates (break Nb–C_σ, Nb–C_π, Nb–O_π; make two Nb–O_σ, C–C_σ) suggest that insertion of coordinated CO_2 into the Nb–R bond to produce the corresponding O-bonded carboxylates also should be thermodynamically feasible. The irreversible nature of the decarbonylation reaction could seal the fate of **1**. Additionally, a kinetic barrier to insertion of **1** may be present because

the observed "outside" orientation of the coordinated CO_2 unit prevents a least motion pathway for migration of R from Nb to the carboxyl carbon (Scheme 2). Alternative migratory insertion via Nb- to O-migration of the alkyl group would produce the thermodynamically less stable metallocarboxylate ester. Least motion migratory insertion to produce the thermodynamically favored O-carboxylate requires isomerization from the "outside" to the "inside" η^2-CO_2 complex, a process which appears to have a substantial activation barrier.

3. Experimental section

3.1. General methods

All reactions were performed under a dry oxygen-free nitrogen or carbon dioxide atmosphere using standard Schlenk and vacuum line techniques. Glassware was oven dried at 120°C overnight prior to use. Hexane, diethyl ether, THF and toluene were purified and dried by refluxing over sodium/benzophenone for 6 h prior to distillation. Me_3CCH_2MgI was prepared by the reaction of Me_3CCH_2I with Mg in diethyl ether. Methylcyclopentadienyl lithium was prepared from the reaction of methylcyclopentadiene monomer with n-BuLi in THF. Cp'_2NbCl_2 and $Cp'_2NbClSiMe_3$ were prepared by published methods [9]. $^{13}CO_2$(99.5%) and $C^{18}O_2$(49.5%) were purchased from ICON Services Inc., NJ. ^1H NMR spectra were recorded at 300 MHz and ^{13}C spectra at 100 MHz. Elemental analyses were performed by Galbraith Laboratories, Inc.

3.2. Preparation of $Cp'_2Nb(CH_2Ph)Cl$

To a suspension of Cp'_2NbCl_2 (1.0 g, 3.1 mmol) was added $ClMgCH_2Ph$ (3.1 ml, 1.0 M in ether) dropwise at 0°C. The mixture gradually turned dark red during addition. The solution was warmed to room temperature and stirred for an additional 3 h. Evaporation of the solvent under reduced pressure, followed by extraction of the residue with warm toluene, gave dark red microcrystals of the title compound in 67% yield on cooling. This material was not characterized but used directly in the preparation of **1c**.

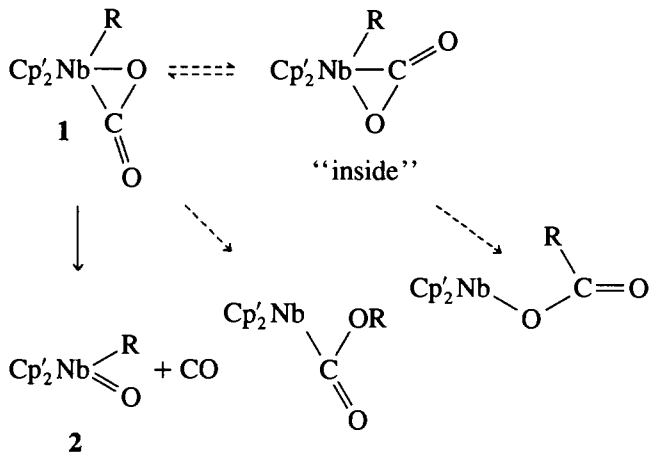

Scheme 2.

3.3. Preparation of Cp'_2NbMe_2

To a suspension of Cp'_2NbCl_2 (3.0 g, 9.3 mmol) was added methyl lithium (6.2 ml, 3.0 M in ether) dropwise at 0°C. After the addition was complete, the flask was warmed to room temperature and the mixture stirred for 2 h. Removal of the solvent at reduced pressure followed by extraction of the residue with warm hexane gave the title compound as a dark red powder in 75% yield on cooling to −10°C.

3.4. Preparation of $Cp'_2Nb(Cl)Me$

To a solution of Cp'_2NbMe_2 (1.20 g, 4.27 mmol) in 25 ml benzene was added $PbCl_2$ (1.19 g, 4.27 mmol). After stirring the mixture for 3 days, the brown solution was filtered to remove precipitated Pb. Evaporation of the filtrate afforded $Cp'_2Nb(Cl)M$ as a brown solid (62%).

3.5. Preparation of $Cp'_2Nb(\eta^2\text{-}CO_2)CH_2SiMe_3$ (1a)

Adapting the procedure of Lappert and coworkers [8], to a degassed stirred suspension of sodium amalgam (0.5%, 1–1.5 mmol) in THF was added a THF solution of $Cp'_2Nb(Cl)CH_2SiMe_3$ (0.32 g, 1.00 mmol) under an atmosphere of CO_2. The mixture became violet-blue in about 5 min, then turned to green after stirring for 1 h. Filtration, removal of the solvent in vacuo, and extraction with toluene gave colorless crystals of the title compound (0.010 g, 0.25 mmol) in 25% yield on cooling at −10°C. IR(KBr, cm^{-1}) 3102(m), 2946(m), 2876(w), 1697(vs), 1493(w), 1456(w), 1382(m), 1245(s), 1166(s), 1119(m), 1075(m), 1043(m), 983(w), 850(vs), 820(s), 726(s), 676(m), 606(w), 567(w). ^1H-NMR(300 MHz, $CDCl_3$): δ 5.98(m, 4H, H-Cp), 5.20(m, 2H, H-Cp), 5.11(m, 2H, H-Cp), 1.62(s, 6H, CH_3-Cp), 1.58(s, 2H, CH_2Si) 0.13(s, 9H, $Si(CH_3)_3$). ^{13}C-NMR(75 MHz, $CDCl_3$): δ 200.9, 119.3, 114.9, 104.9, 96.8, 94.4, 16.1, 14.3, 4.6. MS(12 eV, Dip) m/e(%) 339(M^+-CH_3, 24.8), 338(M^+-CO, 19), 266.9(M^+-CO-CH_2SiMe_3, 29.2), 249.9(M^+-CO_2-CH_2SiMe_3 − 1, 100). UV–visible: λ_{max} = 242 nm (CH_2Cl_2), $\epsilon_{max} = 1.98 \times 10^4$. $Cp'_2Nb(\eta^2\text{-}^{13}CO_2)CH_2SiMe_3$ and $Cp'_2Nb(\eta^2\text{-}C^{18}O_2)CH_2SiM_3$ were obtained by using a $^{13}CO_2$ or $C^{18}O_2$ atmosphere during the final step in preparing **1a**. $Cp'_2Nb(\eta^2\text{-}^{13}CO_2)CH_2SiM_3$: IR(KBr, cm^{-1}) 1654($\nu_{C=O}$); $Cp'_2Nb(\eta^2\text{-}C^{18}O_2)CH_2SiM_3$: IR(KBr, cm^{-1}) 1672($\nu_{C=O}$).

3.6. Preparation of $Cp'_2Nb(\eta^2\text{-}CO_2)CH_2CMe_3$ (1b)

To an excess of sodium amalgam (0.5%) was added a THF solution of $Cp'_2NbClCH_2CMe_3$ (0.32g, 1.00 mmol) under 1 atm CO_2 and the mixture was stirred for 1 h. Filtration, removal of the solvent in vacuo, and extraction with toluene gave colorless crystals of the title compound in 22% yield on cooling at −10°C. IR(KBr, cm^{-1}) 3105(m), 2952(m), 1699(vs), 1654(w), 1495(m), 1457(m), 1384(m), 1359(m), 1169(s), 1127(m), 1106(m), 1074(m), 863(s), 849(m), 732(s). ^{1}H-NMR(300 MHz, $CDCl_3$) δ 6.33(m, 2H, H-Cp), 5.97(m, 2H, H-Cp), 5.24(m, 2H, H-Cp), 5.11(m, 2H, H-Cp), 1.14(s, 9H, $C(CH_3)_3$), 1.12(s, 2H, CCH_2), 1.07(d, 6H, CH_3-Cp); MS(El, 12 eV) *m/e*(%) 338.1(M^+-CO, 11.6), 322.1(M^+-CO_2, 3.4), 266.9(M^+-CO-CH_2CMe_2, 54.8) 249.9(M^+-CO_2-CH_2CMe_3-1, 100). Anal. Calc. (found) for $C_{18}H_{25}NbO_2$: C 59.01 (59.12), H 6.83 (6.96).

3.7. Preparation of $Cp'_2Nb(\eta^2\text{-}CO_2)CH_2Ph$ (1c)

Under an atmosphere of CO_2, $Cp'_2Nb(CH_2Ph)Cl$ (0.62 g, 1.62 mmol) was dissolved in 15 ml THF, and the solution was transferred to a flask containing degassed Na/Hg (excess). After stirring the solution for 1 h, filtration, removal of the solvent under reduced pressure, and extraction of the residue with toluene gave a light yellow solution from which white microcrystals of the title compound were obtained at −10°C (27%). IR(KBr, cm^{-1}) 3098(m), 2959(w), 2901(w), 1704(vs), 1655(w), 1593(s), 1495(m), 1484(m), 1458(m), 1377(m), 1261(s), 1209(m), 1164(s), 1122(s), 1072(m), 1041(w), 1029(w), 851(s), 758(m), 732(s), 705(s). ^{1}H-NMR (300 MHz, $CDCl_3$) δ 7.19(m, 5H, −Ph), 5.78(m, 2H, H-Cp), 5.72(m, 2H, H-Cp), 5.22(m, 2H, H-Cp), 4.99(m, 2H, H-Cap), 2.40(s, 3H,CH_3-Cp), 1.25(s, 2H, $-CH_2Ph$). ^{13}C-NMR(75 MHz, $CDCl_3$) δ 200.6, 153.0, 128.2, 128.3, 123.5, 116.0, 104.6, 99.5, 97.3, 34.0, 12.0. MS(12 eV, DIP) *m/e*(%) 358(M^+-CO, 27.8), 342(M^+-CO_2, 100), 266.9(M^+-CO-CH_2Ph, 76.6), 248.9(M^+-CO_2-CH_2Ph, 93.7). Analysis calculated (found) C 62.18 (61.95); H 5.40 (5.56). $Cp'_2Nb(\eta^2\text{-}C^{18}O_2)CH_2Ph$ and $Cp'_2Nb(\eta^2\text{-}^{13}CO_2)CH_2Ph$ were obtained using $C^{18}O_2$ and $^{13}CO_2$ respectively in the final step of preparing **1c**. $Cp'_2Nb(\eta^2\text{-}^{13}CO_2)CH_2Ph$, IR(KBr, cm^{-1}), 1659($\nu_{C=O}$); $Cp'_2Nb(\eta^2\text{-}^{13}CO_2)CH_2Ph$, IR(KBr, cm^{-1}), 1676($\nu_{C=O}$).

3.8. Preparation of $Cp'_2Nb(\eta^2\text{-}CO_2)CH_3$ (1d)

Under an atmosphere of CO_2, $Cp'_2Nb(CH_2Ph)Cl$ (0.62 g, 1.62 mmol) was dissolved in 15 ml THF, and the solution was transferred to a flask containing degassed Na/Hg (excess). After stirring the solution for 1 h, filtration, removal of the solvent under reduced pressure, and extraction of the residue with toluene gave a light yellow solution from which white microcrystals of the title compound were obtained at −10°C (15%). IR (KBr, cm^{-1}) 3103(w), 2963(m), 2926(m), 2860(w), 1698(s), 1652(w), 1495(w), 1457(w), 1262(s), 1173(m), 1099(s), 1024(s), 801(s), 734(w), 701(w), 569(w). ^{1}H-NMR (300 MHz, $CDCl_3$) δ 5.84 (m, 2H, H-Cp), 5.64(m, 2H, H-Cp), 5.23(m, 2H, H-Cp), 5.18(m, 2H, H-Cp), 1.68(s, 6H, CH3-Cp), 0.199(s, 3H, $-CH_3$). MS(12 eV, DIP) *m/e*(%) 282(M^+-CO, 24.5), 267(M^+-CO-Me, 62.6), 248.9(M^+-CO_2-Me-2, 100).

3.9. Thermolysis of $Cp'_2Nb(\eta^2\text{-}CO_2)CH_2SiMe_3$: $Cp'_2Nb(O)CH_2SiMe_3$ (2a)

A THF solution (5 ml) of **1a** (191 mg, 0.50 mmol) was heated at 60°C with attendant disappearance of **1a** over 5 h (IR monitoring at 1735 cm^{-1}). Evaporation of the solvent, followed by sublimation of the residue at 120°C (10^{-2} mm), gave **2a** as a colorless powder (57 mg, 32%). X-ray quality single crystals were obtained from diethyl ether/hexane. IR(KBr, cm^{-1}) 3087(w), 2958(m), 1507(w), 1250(s), 837(vs), 705(m). ^{1}H NMR (300MHz, $CDCl_3$) δ 5.92 (m, 2H, H-Cp), 5.79 (m, 2H, H-Cp), 5.69(m, 2H, H-Cp), 5.47 (m, 2H, H-Cp), 2.04 (s, 6H, CH_3-Cp), 0.70(s, 2H, CH_2Si), 0.06(s, 9H, $Si(CH_3)_3$). ^{13}C NMR (75 MHz, $CDCl_3$) δ 128.7, 114.5, 110.5, 109.9, 102.9, 31.0, 15.8, 3.5; MS(EI, 12 eV) *m/e*(%) 354.2 (M^+, 4.3), 339.0 (M^+-CH_3, 100), 267.0(M^+-CH_2SiMe_3, 35.3). Analysis Calculated (found) for $C_{16}H_{25}NbOSi$: C 54.2 (53.6), H 7.1 (7.2).

^{1}H NMR studies on the thermolysis of **1a**. In a sealed 5 mm NMR tube **1a** (15 mg, 0.039 mmol) was dissolved in 0.5 ml THF-d_8. The sample was heated at 60°C and monitored by ^{1}H NMR. The spectrum of the solution was recorded every 30 min. The concentration of **1a** was calculated based on integration of the resonance of the methyl protons on the Cp′ ring at 1.62 ppm.

3.10. Thermolysis of $Cp'_2Nb(\eta^2\text{-}CO_2)CH_2CMe_3$: $Cp'_2Nb(O)CH_2CMe_3$ (2b)

A THF solution (3 ml) of **1b** (0.10g, 0.27 mmol) was heated at 60°C under nitrogen. Complex **1b** was consumed in about 5 h as indicated by disappearance of the carbonyl absorption at 1736 cm^{-1}. Removal of the solvent in vacuo, followed by extraction of the residue with toluene, gave **2b** as a colorless powder in 18% yield after recrystallization. IR(KBr, cm^{-1}) 3090(w), 2964(m), 2854(w), 1263(s), 1098(m), 1025(m), 866(w) 803(s). ^{1}H NMR (300 MHz, $CDCl_3$) δ 6.48 (m, 2H, H-Cp), 6.14 (m, 2H, H-Cp), 5.99 (m, 2H, H-Cp), 5.85 (m, 2H, H-Cp), 2.14 (s, 6H, CH_3-Cp), 1.55(s, 9H, $C(CH_3)_3$), 0.91(s, 2H, C-CH_2). MS(EI, 12 eV) *m/e*(%) 338.1 (M^+-CO, 60.4), 266.9(M^+-CO-CH_2CMe_3, 100), 249.8(M^+-CO-CH_2CMe_3-1, 19.3).

3.11. Thermolysis of $Cp'_2Nb(CO_2)CH_2Ph$ (1c): $Cp'_2Nb(O)Ch_2Ph$ (2c) and $Cp'_2Nb(CO)CH_2Ph$ (4c)

A THF solution of **1c** (at concentrations of 8.64×10^{-3} M, 2.59×10^{-2} M, 4.32×10^{-2} M) was heated at 60°C in THF. The reaction progress was monitored continuously by FT-IR and ^{1}H NMR. At a concentration of 8.64×10^{-3} M, after half consumption of **1c**, removal of the solvent, followed by extraction of the residue with toluene, gave **2c** (25%–35%); longer heating resulted in a decrease in the yield. At concentrations of 2.59×10^{-2} M and 4.32×10^{-2} M, both **2c** and **4c** were generated after half consumption of **1c**; the yields were estimated by ^{1}H NMR as 25%(**2c**)/10%(**4c**) and 20%(**2c**)/10%(**4c**) respectively; further heating also caused a reduction in the yield of **2c**, **3c**. **2c**, IR(KBr pellet, cm^{-1}) 3112(w), 2968(m), 2952(w), 2862(w), 1269(m), 1098(s), 1022(m), 801(s). ^{1}H NMR (300 MHz, $CDCl_3$) δ 7.16 (m, 5H, −Ph), 5.92(m, 2H, H-Cp), 5.51(m, 2H, H-Cp), 5.44(m, 2H, H-Cp), 5.35(m, 2H-Cp), 3.05(s, 2H, CH_2Ph), 1.99(s, 6H, CH_3-Cp); MS(12 eV, DIP) m/e(%) 358.0 (M^+, 54.0), 342.1(M^+-O, 4.4), 266.9(M^+-CH_2Ph, 100), 249.8(M^+-CH_2Ph-O-1, 10.2).

3.12. Thermolysis of $Cp'_2Nb(\eta^2\text{-}C^{18}O_2)CH_2Ph$(1c*) (50% labeled)

A THF (5 ml) solution of $Cp'_2Nb(\eta^2\text{-}C^{18}O_2)CH_2Ph$ (30 mg, 0.078 mmol) was heated at 60°C. The starting material was totally consumed in 35 h as indicated by disappearance of the carbonyl absorption of **1c*** at 1712 cm^{-1}. ^{1}H NMR, FT-IR and GC/MS analyses of the solution revealed the formation of $PhCH_2OH$, PhC(O)H, $PhCH_2CH_2Ph$, $PhCH_3$, and butyrolactone. The relative amount of products was estimated by GC/MS. PhCHO and butyrolactone are the major oxygen-containing organic products, constituting about 20%–30% of the ^{18}O labeled portion; the insoluble niobium-containing products and $PhCH_2OH$ accounted for the rest of the ^{18}O.

3.13. Preparation of $Cp'_2Nb(CO)CH_2Ph$ (4c)

To a degassed suspension of sodium amalgam (0.5% w/w, excess) was added a THF solution of $Cp'_2Nb(Cl)CH_2Ph$ (0.62 g, 1.62 mmol) under an atmosphere of CO. The mixture became blue in about 3 min, then turned to green, while stirring for 1 h. Filtration, removal of the solvent in vacuo, and extraction with toluene gave the title compound as an air sensitive green solid in 42% yield on cooling to −10°C. IR (in THF, cm^{-1}) 3098(w), 2974(m), 2858(m), 1892(vs), 1259(m), 1079(vs), 1033(w), 911(s), 804(m), 748(w). ^{1}H-NMR (300 MHz, $CDCl_3$) δ 7.10(m, 5H, -Ph), 4.80(m, 2H, H-Cp), 4.70(m, 2H, H-Cp), 4.25(m, 2H, H-Cp), 4.52(m, 2H, H-Cp), 2.92(s, 2H, CH_2Ph), 1.91(s, 6H, CH_3-Cp). MS(12 eV, DIP) m/e(%) 370(M^+, 0.4), 342(M^+-CO, 37.4), 248.9(M^+-CO-CH_2Ph-2, 100).

3.14. X-ray structure determination of 1c and 2a

Crystals were obtained from diethyl ether/hexane at −10°C. The structures were solved by the heavy atom method and all hydrogen atoms were located and refined isotropically. Calculations were carried out using the SHELXL-76 program. Collection and structure determination data are summarized in Table 2. Tables of atomic coordinates and bond lengths and angles are provided in the Experimental section; tables of thermal parameters and structure factors are provided as Supplementary materials.

Acknowledgments

We are grateful for support provided by the US Department of Energy, Office of Basic Energy Sciences (89ER13997).

References

[1] (a) I.S. Kolomnikov and T.V. Lyskak, *Russ. Chem. Rev.*, *59* (1990) 344.
(b) P. Braunstein, D. Matt and D. Nobel, *Chem. Rev.*, *88* (1988) 747.
(c) A. Behr, in *Carbon Dioxide Activation by Metal Complexes*, VCH, Weinheim, 1988.
(d) D. Walther, *Coord Chem. Rev.*, *79* (1987) 135.
(e) D.J. Darensbourg and R.A. Kudaroski, *Adv. Organomet. Chem.*, *22* (1983) 129.

[2] J.M. Maher and N.J. Cooper, *J. Am. Chem. Soc.*, *104* (1980) 6796.
G.R. Lee, J.M. Maher and N.J. Cooper, *J. Am. Chem. Soc.*, *109* (1987) 2956.

[3] J. Bryan, S.J. Geib, A.L. Reingold and J.M. Mayer, *J. Am. Chem. Soc.*, *109* (1987) 2326.
J.C. Bryan and J.M. Mayer, *J. Am. Chem. Soc.*, *112* (1990) 2298.
H. Alt, K.H. Schwind and M.D. Rausch, *J. Organomet. Chem.*, *321* (1987) C9.

[4] (a) R.L. Harlow, J.B. Kinney and T. Herskovitz, *J. Chem. Soc. Chem. Commun.* (1980) 813.
(b) T. Forschner, K. Menard and A.R. Cutler, *J. Chem. Soc. Chem. Commum.*, (1984) 121.
(c) M.E. Giuseppetti and A.R. Cutler, *Organometallics*, *6* (1987) 970.
(d) D.H. Gibson and T.S. Ong, *J. Am. Chem. Soc.*, *109* (1987) 7191.
(e) D.R. Senn, J.A. Gladysz, K. Emerson and R.D. Larsen, *Inorg. Chem.*, *26* (1987) 2737.
(f) J.M. Maher, G.R. Lee and N.J. Cooper, *J. Am. Chem. Soc.*, *104* (1982) 6797.

[5] T. Ito and A. Yamamoto, *J. Chem. Soc. Dalton Trans.*, (1975) 1398.
T. Tsuda, S-I. Sanada and T. Saegusa, *J. Organomet. Chem.*, *116* (1976) C10.

M. Arestaa and C.F. Nobile, *Inorg. Chim. Acta, 24* (1977) L49.
J. Wu, P.E. Fanwick and C.P. Kubiak, *Organometallics, 6* (1987) 1805.
D.L. DeLaet, R. del Roario, P.E. Fanwick and C.P. Kubiak, *J. Am. Chem. Soc., 109* (1987) 754.

[6] D.J. Darensbourg and A. Rockicki, *Organometallics, 1* (1982) 1685.
E. Klei and J.H. Telgen, *J. Organomet. Chem., 222* (1981) 79.
D.J. Darensbourg, H.P. Wiegreffe and P.W. Wiegreffe, *J. Am. Chem. Soc., 112* (1990) 9252.
D.J. Darensbourg, A. Rokicki and M.Y. Darensbourg, *J. Am. Chem. Soc., 103* (1991) 3223.

[7] (a) K.A. Belmore, R. Vanderpool, J.-C. Tsai, M.A. Khan and K.M. Nicholas, *J. Am. Chem. Soc., 110* (1988) 2004.
(b) J.-C. Tsai, M. Khan and K.M. Nicholas, *Organometallics, 8* (1989) 2967.
(c) J.C. Tsai, M.A. Khan and K.M. Nicholas, *Organometallics, 10* (1991) 29.
(d) P.-F. Fu, M.A. Khan and K.M. Nicholas, *Organometallics, 10* (1991) 382.
(e) J.C. Tsai, R.A. Wheeler, M.A. Khan and K.M. Nicholas, *Organometallics, 10* (1991) 1344.
(f) P.F. Fu, M.A. Khan and K.M. Nicholas, *Organometallics, 11* (1992) 2607.
(g) W. Ziegler and K.M. Nicholas, *J. Organomet. Chem., 423* (1992) C35.

[8] G.S. Bristow, P.B. Hitchcock and M.F. Lappert, *J. Chem. Soc., Chem. Commun.* (1981) 1145.

[9] P.B. Hitchcock and M.F. Lappert, *J. Chem. Soc., Dalton Trans.* (1981) 180.

[10] C. Jegat, M. Fouassier and J. Mascetti, *Inorg. Chem., 30* (1991) 1521, 1530.

[11] R. Alvarez, E. Carmona, J.I. Martin, M.L. Poveda, E. Gutierrez-Puebla and A. Mong, *J. Am. Chem. Soc., 108* (1986) 2286.
E. Carmona, A.K. Hughes, M.A. Munoz, D.M. O'Hare, P.J. Perez and M.L. Poveda, *J. Am. Chem. Soc., 113* (1991) 9210.

[12] P. Fu, M.A. Khan and K.M. Nicholas, *J. Am. Chem. Soc., 114* (1992) 6579.

[13] S.E. Halfon, M.C. Fermin and J.W. Bruno, *J. Am. Chem. Soc., 111* (1989) 5490.
A. Antinolo, A. Otero, M. Fajardo, C. Lopez-Mardomingo, D. Lucas, Y. Mugnier, M. Lanfranchi and M.A. Pellinghelli, *J. Organomet. Chem., 435* (1992) 55.
E.J. Moore, D.A. Straus, J. Armantrout, B.D. Santarsiero, R.H. Grubbs and J.E. Bercaw, *J. Am. Chem. Soc., 105* (1983) 2068.

[14] W.A. Nugent and J.M. Mayer, in *Metal–Ligand Multiple Bonds*, Wiley, New York, 1988, pp. 159–179.

[15] R. Mercier, J. Douglade, J. Amaudrut, J. Sala-Pala and J.E. Guerchais *J. Organomet. Chem., 244* (1983) 145.

[16] O. Eisenstein and U. Paris, Orsay, unpublished results, 1990.

[17] J.A. Martinho Simoes and J.L. Beauchamp, *Chem. Rev., 90* (1990) 629.

[18] G.R. Davies, J.A.J. Jarvis, B.T. Kilbourn and A.J.P. Pioli, *J. Chem. Soc. Chem. Commun.* (1971) 677.
G.R. Davies, J.A.J. Jarvis and B.T. Kilbourn, *J. Chem. Soc. Chem. Commun.* (1971) 1511.
C.J. Cardin, D.J. Cardin, J.M. Kelly, R.J. Norton, T.J. King, H.E. Parge and A. Roy, in G. Wilkinson (ed.), *Comprehensive Organometallic Chemistry*, Vol. 3, Pergamon, London, 1982, p. 594.

[19] A.R. Middleton and G. Wilkinson, *J. Chem. Soc. Dalton Trans.*, (1980) 1888.

[20] A. Antinolo, S. Garcia-Liedo, J. Martinez de Ilarduya and A. Otero. *J. Organomet. Chem., 335* (1987) 85.

[21] A.A. Pasynskii, Y.V. Skripkin and V.T. Kalinnikov, *J. Organomet. Chem., 150* (1978) 51.